DETAILED DESIGN OF A RANKINE VAPOR MICROTURBOPUMP FOR ELEVATED TEMPERATURE OPERATION

Mokhtar Liamini, Félix Gauthier, Philippe Beauchesne-Martel, Luc G. Fréchette
Department of Mechanical Engineering, Université de Sherbrooke, Sherbrooke, Canada

Abstract: This paper presents the design of a microturbopump aimed at operation in a Rankine vapor power cycle with superheated steam. Analytical, numerical models and past experience were used to design the various components specifically for elevated temperature operation, including a radial outflow microturbine, a spiral groove viscous micropump, fluid film bearings and seals. Based also on a previous study of heat and stress management, the final layout of a demonstration device was defined, consisting of seven wafers (silicon, glass/quartz, and silicon-on-insulator) that are microfabricated using techniques such as deep reactive ion etching (DRIE), advanced oxide etching, wet etching, anodic and fusion bonding. This device is the first microturbine design that manages heat flows using insulation materials and strategies, which is an important milestone in achieving efficient and robust micro heat engines.

Keywords: microturbine, micropump, high temperature, design, steam, Rankine, glass, quartz.

INTRODUCTION

In a previous paper presented to PowerMEMS [1], we discussed the heat and stress management in a Rankine steam microturbine in the context of energy harvesting from the exhaust gases of cars. This application sets the design conditions (pressure and temperature) to calculate the Rankine thermodynamic cycle and determine the overall configuration. Based on simplified models concerning losses and efficiencies approximated from past experience, the calculated global configuration consists in four turbines in series, three of them driving generators and the fourth one driving a pump.

The multi-spool configuration has several benefits. It first has the advantage of decreasing the temperature gradients in each device which makes thermal insulation more feasible. Secondly, it permits to divide the number of turbine stages (on the order of 20) on several rotors. And last but not least it allows separating some components like the pump and the generator simplifying hence the design and fabrication of each device.

We focused our interest on the microturbopump since it implies dealing with high temperature gradients on a device containing both liquid and hot steam (See Fig.1). This challenge wasn't faced before in similar concepts and is a milestone for the design of a viable steam microturbine. The device configuration must ensure proper thermal insulation in three locations: 1) across the rotor to prevent the hot steam to heat up the liquid in the pump; 2) between the top and bottom portions of the device to prevent conduction losses from the turbine flow; 3) between the outer radius and the center of the bottom part to maintain steam in the bearings and liquid in the pump. These thermal challenges were previously presented [1], so the focus here is on the detailled device design and fabrication process.

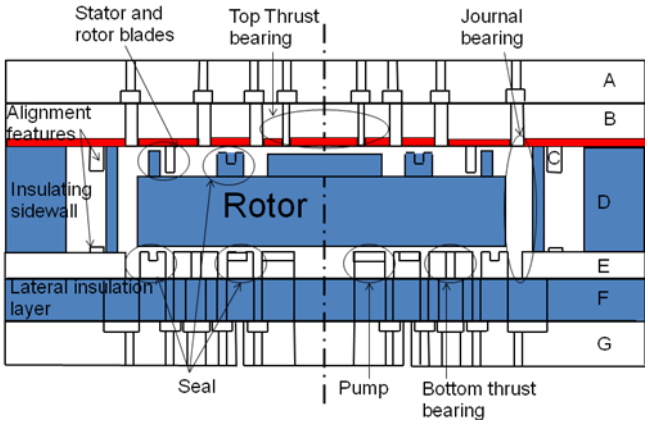

Figure 1: Schematic cross-section of a Rankine Micro turbine. The structure is ~2 mm in thickness and ~15 mm on its side, with a 4 mm diameter rotor.

MICROTURBOPUMP LAYOUT AND FABRICATION

Global layout and assembly

A microturbopump was designed for the experimental demonstration of feasibility for such a device. The overall layout consists in seven layers of Silicon, Glass or Quartz, and Silicon-on-Insulator (SOI) (Fig. 1 and 2), used to implement the required components while providing adequate thermal insulation. The layers A, B and C are bonded together and constitute the top portion of the chip. The layers F, E and G are also bonded together to form the bottom portion of the chip. For the assembly, the

concept is to align the insulating honeycomb layer D on the stack E-F-G thanks to etched mechanical alignment structures present on E and then manually inserting the rotor. Finally, we place the stack A-B-C over the other chips, aligning it with similar alignment structures present on C layer. The whole device is maintained together by an external casing containing tubes for inlet and outlet flows as well as holes in the outermost layers for temperature measurements. A device made entirely in silicon will first be fabricated to validate many components with ambient temperature air and demonstrate the viability of the alignment technique proposed here.

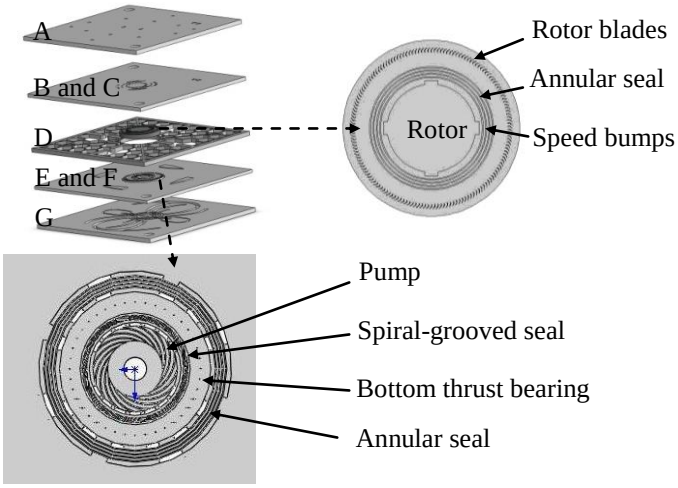

Figure 2: Layers of the microturbopump demo device, in the final version, B is in SOI, D in Pyrex, F in Pyrex. A, C, E and G are in Silicon.

Process flow

The silicon layers are processed following well known microfabrication techniques: deep reactive ion etching (DRIE), fusion and anodic bonding, and wet etching. As a particular feature of this device, the layer C is originally made out of a Silicon-on-Insulator wafer that is first bonded on the layer B with a thin oxide layer as interface. Its handle layer is completely grinded and then we etch the stator blades and alignment structure in the device layer using the flat and clean oxide interface between B and C as an etch stop. This allows later to have an almost perfect surface contact when assembling with layer D.

Another special characteristic of this device is that it will include Pyrex and Quartz layers as insulating barriers. Those layers could be fabricated using ultrasonic machining, although advanced oxide etching (AOE) techniques will be required to achieve the level of tolerances and an accurate control of the verticality and aspects-ratios.

In addition to this, layer F should be made in Pyrex and will serve as a lateral insulation in the bottom side of the device to separate the pump region from the surrounding components that operate with high temperature steam. It imposes that the cold regions in Silicon on layers E and G are separated from the hot ones as "islands". So, the concept used is to etch first the central layer F of Pyrex. Then, the Silicon wafer G is etched from the top and bonded to layer F. Etching layer G from the bottom allows then to create the holes and the desired cold "island". Then, a Silicon-on-Insulator wafer is bonded to the F-G stack to add layer E. Its handle layer is grinded and after etching the various grooves, it is etched till reaching the Pyrex, to form the required "islands" on the top of the E-F-G stack.

DETAILED DESIGN

The design of this demo microturbopump is based on the first generation device developed by Lee et al. [2] and demonstrated with air and water at ambient temperature. The models previously used were improved and adapted for the current design to meet the specification for high temperature operation steam. The final design, presented here, represents a trade-off between:

- Optimal geometries for efficient operation, with special care of the power balance and stability of the rotor.
- Design point targeted for car exhaust energy scavenging application.
- Heat transfer and stress management.
- Constraints imposed by state-of-the-art microfabrication.

In what follows we present a global view on the design of the microturbopump with references to more detailed sources for deeper insight.

Turbine

The turbine modeling [3] is based on the Euler equation using velocity triangles and correlations derived from 2D CFD calculations to model the profile and mixing losses, the deviation, and the heat transfer. Adaptation of losses to account for three dimensional effects and correlation for blockage were derived from analytical relationships. Concerning the heat transfer modeling, it considers a model of laminar developing flow between two plates at low Reynolds number with correlations derived from CFD and it considers compressibility effects which constitutes an interesting progress in microturbines modeling.

The turbine is designed to produce the power required to drive the pump and compensate for the various losses either by friction or by heat transfer. In this device, approximately 50 % of the power produced by the turbine is consumed by the pump and 50 % is consumed as drag by the other components. Figure 3 shows the comparison between the power produced by the turbine and the power consumption from the other components including the pump.

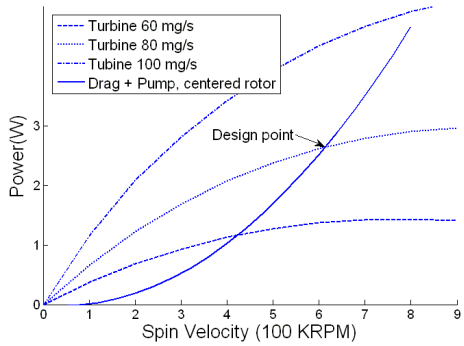

Figure 3: Map of the power delivered by the turbine for several flow rates and comparison with power consumption in the pump and viscous losses.

The operation point is at 600 KRPM and the flow rate of 85 mg/s in the turbine allows the power produced to match the various power consumptions either by drag or by heat transfer. In the eventuality of increasing power consumption, for example in the case of a non-centered rotor, Figure 3 shows the easiness of increasing the power produced simply by increasing the flow rate in the turbine in reasonable limits.

Finally, the calculation of the adequate configuration led to a radial turbine, with only one stage. The stator on the layer C of the device is interdigitated with the rotor on the layer D, providing a configuration that can be extended to multiple blade rows without affecting the device configuration.

Pump

The spiral groove pump used in this device was previously used and demonstrated by Lee et al. [2]. The modeling is based on the Reynolds lubrication equation and the pump is optimized to produce 7.5 atm of pressure rise while delivering ~ 70 mg/s of mass flow rate with an optimal efficiency (see fig.4). The maximum mass flow it can deliver while opening the outlet is 85 mg/s and the maximum pressure rise is ~ 4.5 MPa. To be fully compatible with the multi-spool configuration calculated for the car exhaust energy scavenging application, the pump should deliver 80 mg/s with a pressure rise of 3 MPa.

The design presented here doesn't respect those specifications but represents an important step toward it.

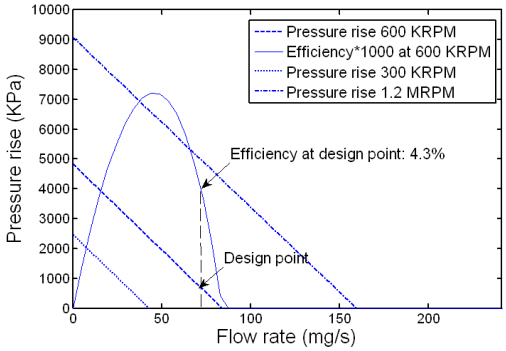

Figure 4: Pump ma of pressure rise versus mass flow rate for three different speeds.

It represents however an important step toward a fully functional autonomous device.

Thrust bearings

The current device comports two thrust bearings, one on the top (turbine side) and one in the bottom (pump side). This configuration gives several advantages compared to a configuration with a single thrust bearing. First it enhances the axial control of the rotor especially in this case where the force in the turbine region is far smaller than the force in the pump region at the design point. Secondly, it allows determining the axial position of the rotor by using one of the thrust bearings as a measurement device by characterizing its pressure variation versus mass flow rate according to the gap with the rotor.

The thrust bearings were modeled as fluidic resistances that were calculated either analytically or using CFD. The models were previously used by Lee et al. [2] and improved/validated by Gauthier [4]. The optimization of the thrust bearings was done to provide the necessary force while minimizing the mass flow rate and the power consumption. The bearings were also checked in the various situations concerning static and dynamic stability. This design is suitable to ensure the axial stability of the rotor in most of the situations during operation; the only exception is with closed pump outlet. In the latter, the force created in the bottom of the rotor is too important to be sustained by the top thrust bearing, so at high speed operation the pump outlet will never be closed completely.

Journal bearing

The journal bearings have been a major interest in this kind of device in the past years [5]. Not much change was done on the journal bearing except that, based on recent work by Lixian Liu [6], an

asymmetric 4-plenums journal bearing was preferred for important improvement of stability.

Seals

Three seals are used in this device: a)an annular seal, separating top thrust bearing outlet from the turbine inlet, b)a spiral partially grooved seal in the bottom separating the pump inlet form the bottom thrust bearing inner outlet, and c) an annular seal separating the bottom thrust bearing outer outlet from the journal bearing inlet. The annular seals consist simply in successive annular grooves alternating with narrow gap zones creating high fluidic resistances that can sustain a high pressure gradient with very low flow rate [7]. The model used was a simple pseudo-compressible laminar flow. The model used for the spiral-grooved seal is similar to that of the pump [2] and the target here is to face the possible pressure rise created by the centrifugal forces in the pump inlet due to the spinning disk.

CONCLUSION

For the first time, a microturbopump using steam as the working fluid is being developed. This implies novel approaches for thermal insulation and hence materials other than silicon that must be microfabricated and integrated. The expected performance and stability should also benefit from the improvements in modelling and design, such as the bearing and seal configuration. The masks are now ready to start the fabrication of the first demo device. Demonstrating such a device will be a very important step toward the development of a viable steam microturbine for a wide range of scientific and industrial applications. The following table presents the main characteristic geometries.

Turbine			
Type	1 stage planar radial outflow , NACA A3K7	Stator chord	185µm
Outer radius	2 mm	Rotor chord	109µm
Solidity	1.5	Blade height	80µm
Design angles Stator	L.E. : 0, T.E. : 72.8	Design angles rotor	L.E. : 50,T.E. :-54
Pump			
Type	Spiral Groove Viscous	Spiral angle (deg.)	16
Radial extent	Ri: 600µm, Ro: 920µm	Groove depth	4.5 µm
Groove Number	16	Circumferential Ratio of ridge to groove	0.3
Design gap	0.5µm	Gap range	0-1µm
Partially Grooved Seal			
Type	Partially spiral grooved	Spiral angle (deg.)	16
Radial extent of grooved part	Ri: 1050µm, Ro: 1150µm	Radial extent of flat part	Ri: 1000µm, Ro:1050µm
Groove number	40	Circumferential Ratio of ridge to groove	1
Design gap	0.5µm	Design operating gap range	0-1µm
Design gap		0.5um	

Journal Bearing			
Type	Hydrostatic axial flow , asymmetric	Gap	15µm
Length	300 µm	Feed plenum layout	4×80°
Top Thrust Bearing			
Type	Hydrostatic	Diameter of capillary	11µm
Number of capillary	40	Radial position of capillary	900µm
Length of capillary	100µm	Radial extent of restrictor	Ri: 0µm, Ro: 1000µm
Design gap	1.5 µm	Gap range	0.5-2µm
Bottom and Top Annular Seals			
Type	Annular , hydrostatic	Width of ridges	25µm
Number of grooves	3	Gap range	0-1µm
Design gap	0.5µm	Groove depth	4.5µm
Bottom Thrust Bearing			
Type	Hydrostatic	Diameter of capillary	12um
Number of capillary	40	Position of capillary	1425um
Length of capillary	100µm	Radial extent of restrictor	Ri: 1200µm, Ro:1650µm
Design gap	1.5µm	Gap range	0.5-2µm

ACKNOWLEDGMENTS

This work was supported by the National Sciences and Engineering Research Council (NSERC) of Canada and General Motors of Canada through Carlton Fuerst. The authors want to thank Prof. Srikar Vengallatore and Hassan Shahriar for their helpful discussions and suggestions.

REFERENCES

[1] M Liamini et al., “Thermal and Structural Considerations in the Design of a Rankine Vapor Microturbine” *Proc. MEMS 2008,* pp. 100-103.

[2] C Lee et al., “Design, Fabrication and Characterization of a microturbopump for a Rankine Cycle Micro Power Generator”, *Proc. 2006 Solid State Sensor, Actuator and Microsystem Workshop.*

[3] P B-Martel et al., “Aerothermodynamics of Sub-Millimiter-Scale Microturbomachinery: Numerical Analysis and Modeling Principles”, *Proc. IMECE 2008, ASME.*

[4] F Gauthier et al., “Achieving Axial Balance of a Microturbine Rotor with Low Bearing Pressures for Start-up and High Speed Operation”, International Workshop on Micro and Nanotechnology. Berkeley, California, 2006.

[5] Fréchette, L.G. et al.,"High-Speed Microfabricated Silicon Turbomachinery and Fluid Film Bearings". *J. Microelectromechanical Systems*, Vol. 14, No.1, 2005.

[6] L Liu, “Theory for Hydrostatic Gas Journal Bearings for Micro-Electro-Mechanical Systems”, MIT PHD Thesis, 2005.

[7] C J Teo, “MEMS Turbomachinery Rotordynamics: Modeling, Design and Testing”, MIT PHD Thesis, 2006.